Hindawi
Advances in Civil Engineering
Volume 2022, Article ID 4529993, 13 pages
https://doi.org/10.1155/2022/4529993

Research Article

Static Mechanical Properties and Microscopic Analysis of Hybrid Fiber Reinforced Ultra-High Performance Concrete with Coarse Aggregate

Shengbing Liu and Yonglei Zhang

School of Civil Engineering and Architecture, Wuhan Institute of Technology, Wuhan 430074, China

Correspondence should be addressed to Shengbing Liu; liushengbing@wit.edu.cn

Received 15 July 2022; Revised 27 September 2022; Accepted 8 October 2022; Published 26 October 2022

Academic Editor: Anush Chandrappa

An orthogonal test was conducted to investigate the effect of hybrid fiber on the mechanical properties of ultra-high performance concrete (UHPC-CA) with coarse aggregate . It was used to design and manufacture 144 test specimens for compressive strength, flexural tensile strength, static compressive elastic modulus test, and SEM microscopic test. Considering the mass replacement rate of coarse aggregate (10%, 15%, 20%, and 30%), the steel fiber volume rate (0%, 0.5%, 1.0%, and 1.5%), and the polypropylene fiber volume rate (0%, 0.05%, 0.10%, and 0.15%). The results show that the volume fraction of steel fiber has the greatest impact on compressive strength and flexural tensile strength, followed by the mass substitution rate of coarse aggregate, and the volume fraction of polypropylene fiber has the smallest impact. For the elastic modulus under static compression, the mass substitution rate of coarse aggregate has the greatest impact, followed by the volume fraction of steel fiber and polypropylene fiber. Based on the analysis of compressive properties, flexural tensile properties, and elastic modulus, the optimal mix ratio is recommended as follows: coarse aggregate 15%, steel fiber 1.5%, and polypropylene fiber 0.10%. Finally, three kinds of strength parameters are predicted based on the back propagation (BP) neural network system. The absolute value of the relative error between the predicted strength and the experimental value is less than 5%, which indicates that the prediction model proposed in this paper can provide a reference for the multiobjective optimization of the mix proportion of hybrid fiber ultra-high performance concrete.

1. Introduction

Ultra-highperformance concrete (UHPC) is a new type of cement-based material with high strength, high durability, high toughness, super chemical corrosion resistance, and low porosity. However, a low water-binder ratio leads to high material and production costs of UHPC. Compared with ordinary UHPC, the cost for ultra-high performance concrete (UHPC-CA) containing coarse aggregate has been greatly reduced. Through the statistics of the cost of general reactive powder concrete (RPC) by researchers, it is found that the cost generally reaches CNY 4000/m^3, and even some costs are as high as CNY 8000/m^3, much higher than the price of ordinary concrete [1–3]. With the addition of coarse aggregate, it can reduce the use of cementitious materials to a certain extent, reduce early autogenous shrinkage, and reduce costs. Studies have found that the measured strain and shrinkage values of the UHPC matrix decrease with the increase of aggregate content, and the shrinkage of the UHPC matrix with 605 kg/m^3 coarse aggregate is only 67.6% of that without coarse aggregate [4]. As early as the 1980s, some scholars in China began to consider the application of hybrid fiber composites (HC), and found that hybrid materials had excellent performance and good economy [5]. Through the uniaxial cyclic compression test of concrete specimens, Xu et al. found that hybrid fiber can obviously improve the cyclic mechanical behavior through the constraint effect [6]. It is found that the incorporation of steel fiber and polypropylene fiber into recycled concrete improves the flexural toughness of the recycled concrete matrix significantly, and the flexural toughness increases the most when the content is 1.0% and 0.9%, respectively [7]. Libre

et al. found that steel fiber had the largest increase in the external fiber, which could significantly improve the compressive strength, flexural strength, and fracture performance of concrete [8]. Polypropylene fiber can make concrete strain harden in the early fracture process by toughening. The existing literature [9–11] shows that the increase in the number of fibers will affect the uniform distribution of fibers, weakening the crack resistance and toughening effect, and that the orientation of fibers can be improved by the flow control method. With the decrease of the fiber orientation tensor, the tensile strength of UHPC also shows a trend of decreasing first and then increasing. The samples with the main fiber orientation perpendicular to and parallel to the loading direction show the highest and lowest dynamic characteristics, respectively. Deng et al. [12–14] also mixed steel fibers with two kinds of high-performance synthetic fibers and different scales of steel fibers into the ultra-high performance concrete matrix to explore the variation law of toughness under different hybrid modes and different fiber contents. On the basis of previous research results on ultra-high performance concrete, this paper will focus on the goal of reducing the production cost of ultra-high performance concrete and try to add different amounts of coarse aggregate and steel-polypropylene hybrid fiber to study the influence of various materials on the compressive strength, flexural strength, and elastic modulus of UHPC. The experimental results are analyzed from the microscopic direction, and the experimental results are predicted based on the BP neural network system.

2. Materials and Methods

2.1. Test Raw Materials. The raw materials used in this paper are suitable for practical engineering. The natural river sand in Hubei Province with a fineness modulus of 2.55, ordinary portland cement (P. O52.5), and natural limestone coarse aggregate with a particle size of 4.75–15 mm are used for mix design. The fibers are copper-plated parallel steel fiber (SSF) and polypropylene fiber (PPF), and their performance properties are shown in Table 1. The fly ash is grade 1 fly ash sold by Wuhan Hanyang Zhongcun Concrete Products Co., Ltd.; the silica fume is produced by Henan Yixiang New Materials Co., Ltd. The average particle size is 0.1 μm, the specific surface area is 19100 m^2/kg, and the SiO_2 content is more than 96%. The water-reducing agent is a polycarboxylate superplasticizer with a water reduction rate of ≥37%; the mixed water is ordinary tap water. In order to study the mechanical properties of ultra-high performance concrete containing coarse aggregate, 16 groups of experimental mix proportions were designed by an orthogonal test method. Reference standard T/CBMF 37-2018, the reference mix design is based on UHPC total bulk density 2500 kg/m^3, as shown in Table 2.

2.2. Orthogonal Experiment Design. According to L_{16} (4^5) orthogonal table design three factors, four-level orthogonal test(see Table 3), the mass content of coarse aggregate is based on 2500 kg, which replaces the weight of UHPC mortar by 10%, 15%, 20%, and 30%, respectively. Steel fiber volume fractions of 0, 0.5%, 1.0%, and 1.5%; polypropylene fiber volume ratios of 0, 0.05%, 0.1%, and 0.15%. The specimens used in the experiment were 100 mm × 100 mm × 100 mm and 100 mm × 100 mm × 300 mm. Each group consists of three specimens, for a total of 16 groups. The specimens were prepared by the standard test method after standard maintenance for 28 days.

2.3. Test Method. In this experiment, the production process of ultra-high performance concrete containing coarse aggregate (UHPC-CA) was selected by a forced concrete mixer, strictly in accordance with the standard T/CBMF 37-2018. © mixing time was controlled within 20 min, and the standard room temperature maintenance was adopted. In strict accordance with the requirements of the GB/T50081-2019 standard, the test block was vibrated and covered with plastic film, and the test mold was removed within 48 h. Then, the test block was weighed and numbered, and immediately placed in the relative humidity of 98% at a constant temperature of 20 ± 2°C in the maintenance room for 28 d. The compressive strength was tested by an SYE-2000A pressure testing machine with a range of 0-2000 kN. Four-point bending and static elastic modulus tests using WAW-600, a universal material testing machine, measuring a range of 0–600 kN. The instrument used for the SEM electron microscope test was a scanning electron microscope with a resolution of 3.2 nm and a magnification of 19–300000, which was continuously adjustable and equipped with a secondary electron and backscatter detector. The loading of this test is strictly in accordance with (GB/T 50081) [15]. The ordinary concrete mechanical properties test standard. The loading schematic diagram is shown in Figure 1, and the measured strength value is recorded.

3. Results and Discussion

3.1. Failure Process and Failure Pattern. The failure characteristics of cube compressive strength and the four-point flexural strength test are shown in Figure 2. It was found that the plastic UHPC specimen showed obvious brittle failure. In the loading process of the test, the initial crack was formed at the weak point of the specimen, and then quickly extended to the top of the specimen. The toughness was poor, and obvious brittle failure occurred. For the cube compressive specimen, it was spalling failure along the surrounding, and for the four-point bending specimen, it was suddenly broken into two sections. In the process of cube compressive loading, with the increase of pressure, the crack develops along the weak part of the specimen. When the specimen is loaded to a certain stage with a loud noise, the specimen is completely destroyed, and visible cracks are produced along the sides of the four corners of the cube specimen, but no concrete peeling occurs. In the process of bending loading, with the increase of pressure, the first microcrack appears at the mid-span position at the bottom of the specimen. As the load continues to increase, the crack develops upward. Due to the existence of fiber, the specimen is not broken into two

Table 1: Fiber properties.

Fabric type	Diameter (mm)	Length to diameter ratio	Density (kg/m^3)	Tensile strength (Mpa)	Elastic modulus (GPa)	Extension at break (%)
SSF	0.2	70	7850	2930	210	3.3
PPF	0.04	350	910	400	4.0	26.8

Table 2: Test the benchmark mix ratio.

Category	Cement (kg/m^3)	Silica fume (kg/m^3)	Flyash (kg/m^3)	Water (kg/m^3)	Water reducing admixture (kg/m^3)	Sand (kg/m^3)
	700	150	150	160	30.5	1220

Table 3: Orthogonal table.

Ode	Factor name	Level 1	Level 2 (%)	Level 3 (%)	Level 4 (%)
A	Fiber volume fraction	0	0.50	1	1.50
B	Volume fraction of polypropylene fiber	0	0.05	0.1	0.15
C	Mass content of coarse aggregate	10%	15	20	30

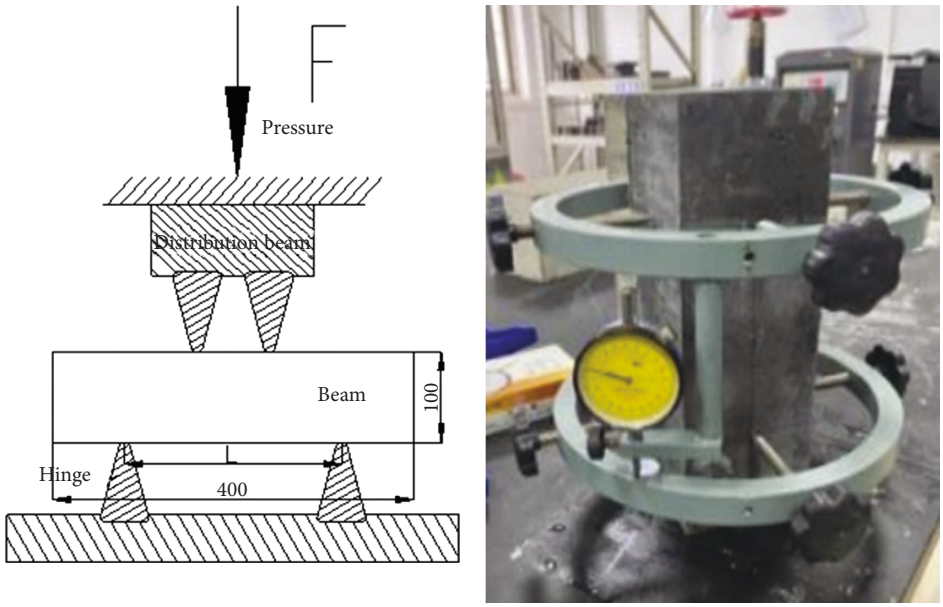

(a) (b)

Figure 1: (a) Loading schematic diagram of bending strength; and (b) diagram of elastic modulus hoop.

sections. On the fracture surface of the specimen, it can be clearly seen that steel fiber and polypropylene fiber are pulled out or broken. The existence of fiber plays a role in bridging cracks, inhibiting crack development, and toughening.

3.2. Test Results. The cube compressive strength, four-point bending strength, and elastic modulus of the test block under various factors are summarized in Table 4.

3.3. Range Analysis. The experimental results in Table 4 are processed to obtain the range analysis table as shown in Table 5, and the intuitive analysis diagram of factors is drawn, as shown in Figure 3.

It can be seen from Table 5, the most influential factor for cube compressive strength and flexural strength is *C* steel fiber, while for the three strength parameters, the influence level of steel fiber is $K4 > K3 > K2 > K1$, that is, the optimal factor level is $K4$. In terms of elastic modulus alone, the influence of factor *A* on coarse aggregate is the most obvious, followed by the *C* steel fiber. The more the content of coarse aggregate is, the greater the elastic modulus is. In terms of cube compressive strength and flexural strength, the optimal factor level of factor *A* is $K2$. In terms of compressive strength and flexural strength, $K2$ is the optimal dosage of factor *A*. For *B* polypropylene fiber, when the factor level is $K3$, the corresponding cube compressive strength and flexural strength reach their maximum at the same time, but

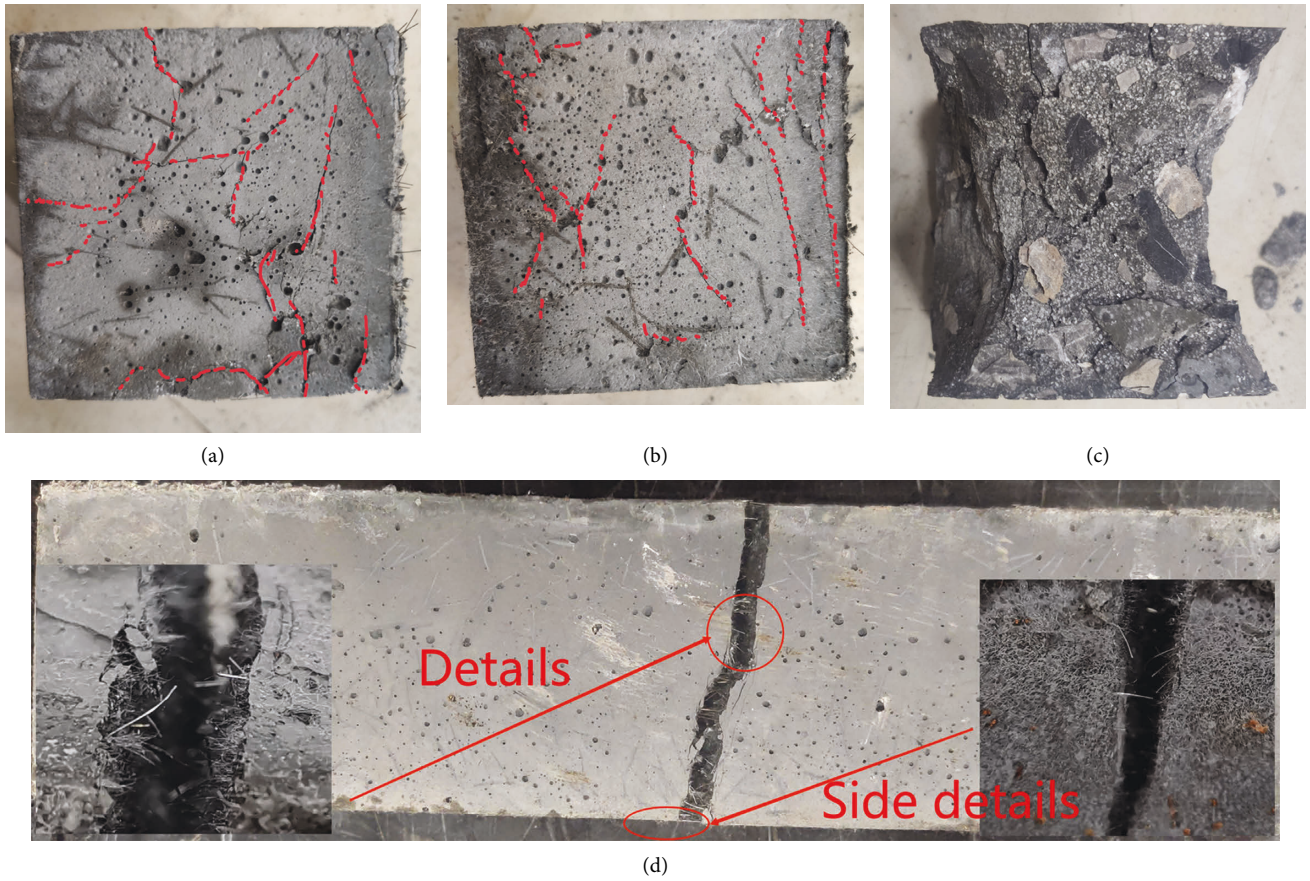

Figure 2: (a) (b) are the compressive failure modes of cubes with different fiber contents; (c) is the compressive failure mode of plain UHPC cubes without fiber; and (d) is the flexural failure mode of UHPC with coarse aggregate hybrid fiber.

Table 4: Summary of experimental results of various factors.

Numbering	A m_{CA} (%)	B v_{PPF} (%)	C v_{SF} (%)	$B \times C$	$f_{cu,k}$ (MPa)	f_{cf} (MPa)	E_c (GPa)
A1	1 (10%)	1 (0)	1 (0%)	1	92.53	11.13	42.1
A2	1 (10%)	2 (0.05%)	2 (0.5%)	2	106.3	16.4	43.5
A3	1 (10%)	3 (0.1%)	3 (1.0%)	3	114.4	19.4	44.8
A4	1 (10%)	4 (0.15%)	4 (1.5%)	4	121.7	20.1	45.1
A5	2 (15%)	1 (0)	2 (0.5%)	3	115.6	14.5	48.5
A6	2 (15%)	2 (0.05%)	1 (0%)	4	101.9	13.2	47.1
A7	2 (15%)	3 (0.1%)	4 (1.5%)	1	136.4	19.8	48.9
A8	2 (15%)	4 (0.15%)	3 (1.0%)	2	125.7	17.6	49.7
A9	3 (20%)	1 (0)	3 (1.0%)	4	121.9	16.7	50.3
A10	3 (20%)	2 (0.05%)	4 (1.5%)	3	129	17.3	51.3
A11	3 (20%)	3 (0.1%)	1 (0%)	2	101	12.8	49.1
A12	3 (20%)	4 (0.15%)	2 (0.5%)	1	108.3	12.9	49.5
A13	4 (30%)	1 (0)	4 (1.5%)	2	127.3	14.5	52.3
A14	4 (30%)	2 (0.05%)	3 (1.0%)	1	123.5	13.1	51.7
A15	4(30%)	3(0.1%)	2 (0.5%)	4	113.1	12.2	50.8
A16	4 (30%)	4 (0.15%)	1 (0%)	3	85.5	10.3	49.2

Note.: m_{CA}, v_{PPF}, an d v_{SF} are the mass content of coarse aggregate, volume content of polypropylene, and steel fiber; $f_{cu,\,k}$, f_{cf}, and E_c are the cube compressive strength, flexural tensile strength, and elastic modulus of concrete block.

they have little effect on the elastic modulus, which is the same as the results described in Reference [16]. Therefore, the optimal mix ratio obtained by range analysis is A2B3C4, that is, the mass content of coarse aggregate is 15%, the volume content of polypropylene is 0.1%, and the volume content of steel fiber is 1.5%.

Through the comparison of the three figures, it can be seen that the influence of the content of coarse aggregate on

Table 5: Range analysis table.

Index	Level	Factor *A* Coarse aggregate	Factor *B* Polypropylene fiber	Factor *C* Steel fiber
Cube crushing strength (MPa)	*K*1	108.73	114.33	95.23
	*K*2	119.90	115.18	110.83
	*K*3	115.05	116.23	121.38
	*K*4	112.35	110.30	128.60
	R	11.17	5.93	33.37
Bending strength (MPa)	*K*1	16.76	14.21	11.86
	*K*2	16.28	15.00	14.00
	*K*3	14.93	16.05	16.70
	*K*4	12.53	15.23	17.93
	R	4.23	1.84	6.07
Static compressive elastic modulus (GPa)	*K*1	43.88	48.30	46.88
	*K*2	48.55	48.40	48.08
	*K*3	50.05	48.40	49.25
	*K*4	51.00	48.38	49.40
	R	7.13	0.10	2.53

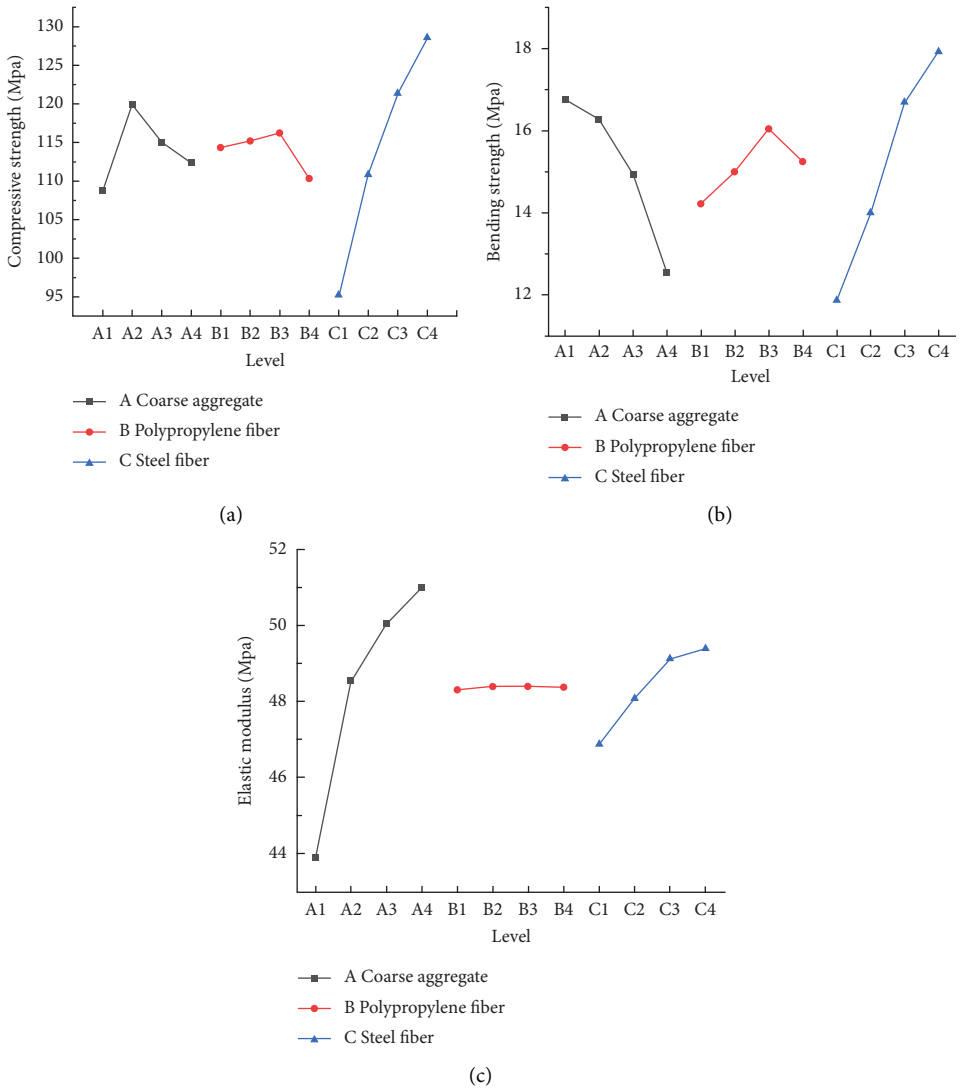

Figure 3: Influence of various factors on different strength parameters; (a) compressive strength; (b) bending strength; and (c) elastic modulus.

the cube compressive strength increases first and then decreases, the influence on the elastic modulus increases gradually, and the influence on the flexural strength obviously decreases. When the content of coarse aggregate is small, the coarse surface can strengthen the interlocking effect of mutual accumulation between aggregates and improve the cube compressive strength, which is 10.3% higher than that of the control group. With the increase of coarse aggregate content, the elastic modulus gradually increases, and it can be seen from the figure that the elastic modulus curve increases linearly. When the mass content of coarse aggregate is 15%, 20%, and 30%, respectively, compared with the 10% group, it increased by 10.6%, 14.1%, and 16.2%. The influence curves of polypropylene fiber on the compressive and flexural properties both increased first and then decreased. Compared with the blank control, the flexural strength increased by 5.6%, 12.9%, and 7.2%, respectively, when the dosage was 0.05%, 0.1%, and 0.15%. Its effect on the elastic modulus is negligible. It can be clearly seen that the addition of steel fibers significantly improved the compressive strength, flexural strength, and elastic modulus of the UHPC-CA matrix. Compared with the 0% content, when the content was 1.5%, the compressive strength, flexural strength, and elastic modulus increased by 35.0%, 51.2%, and 5.4%, respectively.

3.4. Factor Weight Analysis. Compared with the subjective weight method, the entropy weight method reduces the influence of subjective factors, reduces the calculation error, and makes the calculation results more scientific [17, 18]. Based on the AHP and entropy weight methods, this paper analyzes the weight of each factor level and obtains the weight of each factor level by using SPSS software as shown in Table 6. It can be seen from the table that the weight of the three factors on the cube's compressive strength is steel fiber (0.6613) > coarse aggregate (0.2213) > polypropylene (0.1174); the weight of influence on flexural strength was steel fiber (0.4997) > coarse aggregate (0.3486) > polypropylene (0.1517) ; the weight of the elastic modulus is: coarse aggregate (0.7307) > steel fiber (0.2590) > polypropylene (0.0103), which is completely consistent with range analysis.

3.5. Variance Analysis. The variance analysis is shown in Table 7. It can be seen from the table that for UHPC-CA cube compressive strength, the influence of factor *C* steel fiber volume ratio and factor *A* coarse aggregate content is highly significant, while the influence of factor *B* polypropylene fiber is small. For UHPC-CA bending strength, the influence of factor *C* steel fiber volume fraction and factor *A* coarse aggregate content is highly significant, and the influence of factor B polypropylene fiber is also significant. For the elastic modulus of UHPC-CA, the influence of factor C steel fiber volume fraction and factor *A* coarse aggregate content is highly significant, and the influence of factor *B* polypropylene fiber is negligible.

3.6. Analysis of Fiber Mixing Effect. In this paper, the fiber hybrid effect coefficient is used to measure the hybrid effect of steel fiber and polypropylene fiber on three strength parameters. The strength enhancement factor β is introduced, as shown in the following formula :

$$\beta_f = \frac{f_{cpf}}{f_{cp}}. \tag{1}$$

f_{cpf} is fiber-reinforced concrete strength parameters, whereas f_{cp} is plain concrete strength parameters. The hybrid effect coefficient of flexural strength and elastic modulus of PPF-SF hybrid fiber on the cube compressive strength of ultra-high performance concrete containing coarse aggregate is defined as shown in the following formula . When $\alpha > 1$, it shows a positive hybrid effect. When $\alpha < 1$, it shows a negative hybrid effect. Table 8 lists the relationship between the strength enhancement coefficient, hybrid effect coefficient, and fiber content calculated by 16 groups of experimental data in this experiment.

$$\alpha = \frac{\beta_{c-p}}{\beta_c \times \beta_p}. \tag{2}$$

It can be seen from Table 8 that the hybrid fiber added to the coarse aggregate concrete matrix shows a negative hybrid effect for the elastic modulus regardless of the hybrid mode and dosage. For flexural strength and compressive strength, there are both positive hybrid effects and negative hybrid effects. When the two kinds of fibers are mixed, the growth of various strengths is not a simple superposition of single-fiber concrete strength but a hybrid effect. When PPF content is 0.15% and SF content is greater than 0.5%, CA-UHPC shows a positive hybrid effect, and when PPF content is not greater than 0.1% and SF content is 0.5%, CA-UHPC shows a negative hybrid effect. When SF was added alone, the optimal dosage was 1.5%; when PPF was added alone, the optimal dosage was 0.05%. When CF and PPF are mixed, the optimum dosage is 1.5% and 0.1%, respectively. It can be seen that the optimum dosage of single mixing and mixing is not the same, so the mixing effect is not a simple addition of a single mixing effect. The positive hybrid effect between PPF and SF fibers has played a toughening and crack resistance effect in the loading process of concrete, which significantly improves the loading performance of concrete. However, when the fiber content exceeds a certain range, the spacing between fibers decreases, and the fibers overlap and interfere with each other, resulting in a negative hybrid effect [19, 20].

3.7. Microscopic Analysis. In this paper, the bonding effects of coarse aggregate, polypropylene fiber, and steel fiber on the UHPC matrix were observed and analyzed by SEM, and the effects of coarse aggregate, polypropylene fiber, and steel fiber on the UHPC matrix were analyzed and verified. By observing the scanning diagram of the transition zone between coarse aggregate and UHPC matrix in Figures 4(a) and 4(b), it can be seen that the adhesion between coarse aggregate and UHPC matrix is very close, and the thickness of the transition zone is very small, which shows that the full

Table 6: Factor weight analysis table.

Factor	Cube crushing strength			Bending strength			Static compressive elastic modulus		
	Factor weight	Level	Weights of each level	Factor weight	Level	Weights of each level	Factor weight	Level	Weights of each level
A	0.2213	*A*1	0.0422	0.3486	*A*1	0.1541	0.7307	*A*1	0.2799
		*A*2	0.0476		*A*2	0.0820		*A*2	0.1435
		*A*3	0.0384		*A*3	0.0636		*A*3	0.1071
		*A*4	0.0931		*A*4	0.0488		*A*4	0.2002
B	0.1174	*B*1	0.0289	0.1517	*B*1	0.0204	0.0103	*B*1	0.0044
		*B*2	0.0202		*B*2	0.0158		*B*2	0.0033
		*B*3	0.0246		*B*3	0.0501		*B*3	0.0014
		*B*4	0.0437		*B*4	0.0654		*B*4	0.0011
C	0.6613	*C*1	0.3669	0.4997	*C*1	0.0855	0.2590	*C*1	0.0753
		*C*2	0.0818		*C*2	0.1116		*C*2	0.0658
		*C*3	0.0907		*C*3	0.1649		*C*3	0.0557
		*C*4	0.1219		*C*4	0.1377		*C*4	0.0623

Table 7: Variance analysis table.

Index	Factor	SS	DOF	MS	F	Fa (3, 6)	
Cube crushing strength	*A*	266.39	3.00	88.80	11.83	0.01 9.78	2
	B	80.34	3.00	26.78	3.57	0.05 4.76	3
	C	2519.87	3.00	839.96	111.90	0.1 3.29	1
	Error	45.04	6.00	7.51	—	—	—
Bending strength	*A*	12.91	3.00	4.30	23.01	0.01 9.78	2
	B	4.94	3.00	1.65	8.81	0.05 4.76	3
	C	63.16	3.00	21.05	112.52	0.1 3.29	1
	Error	1.12	6.00	0.19	—	—	—
Static compressive elastic modulus	*A*	121.63	3.00	40.54	320.09	0.01 9.78	1
	B	0.00	3.00	0.00	0.01	0.05 4.76	3
	C	16.62	3.00	5.54	43.72	0.1 3.29	2
	Error	0.76	6.00	0.13	—	—	—

Table 8: Strength enhancement coefficient and hybrid effect coefficient of hybrid fibers.

Specimen types(PiSj)	β_{fc}	α_c	β_{ft}	α_t	β_{Ec}	α_E
P0S0	1.00	1.00	1.00	1.00	1.00	1.00
P0S0.5	1.25	1.00	1.30	1.00	1.15	1.00
P0S1.0	1.32	1.00	1.50	1.00	1.19	1.00
P0S1.5	1.38	1.00	1.30	1.00	1.24	1.00
P0.05S0	1.10	1.00	1.19	1.00	1.12	1.00
P0.05S0.5	1.15	0.83	1.47	0.95	1.03	0.80
P0.05S1.0	1.33	0.92	1.18	0.66	1.23	0.92
P0.05S1.5	1.39	0.92	1.55	1.01	1.22	0.88
P0.1S0	1.09	1.00	1.15	1.00	1.17	1.00
P0.1S0.5	1.22	0.90	1.10	0.73	1.21	0.90
P0.1S1.0	1.24	0.86	1.74	1.01	1.06	0.76
P0.1S1.5	1.47	0.98	1.78	1.19	1.16	0.80
P0.15S0	0.92	1.00	0.93	1.00	1.17	1.00
P0.15S0.5	1.17	1.01	1.16	0.96	1.18	0.87
P0.15S1.0	1.36	1.12	1.58	1.14	1.18	0.85
P0.15S1.5	1.32	1.03	1.81	1.50	1.07	0.74

Note.: PiSj, where i and j are the volume contents of polypropylene and steel fiber, respectively; β_{fc}, β_{ft}, and β_{Ec} are the compressive strength, flexural strength, and the strength enhancement coefficient of the elastic modulus under hybrid fiber, respectively; α_c, α_t, and α_E are the hybrid effect coefficients of the three, respectively.

contact between the rough aggregate surface area and the concrete matrix makes the width of microcracks at the transition interface close to 0, which is significantly improved compared with ordinary concrete. There are two reasons for the influence of coarse aggregate on the performance of UHPC. First, the surface roughness can

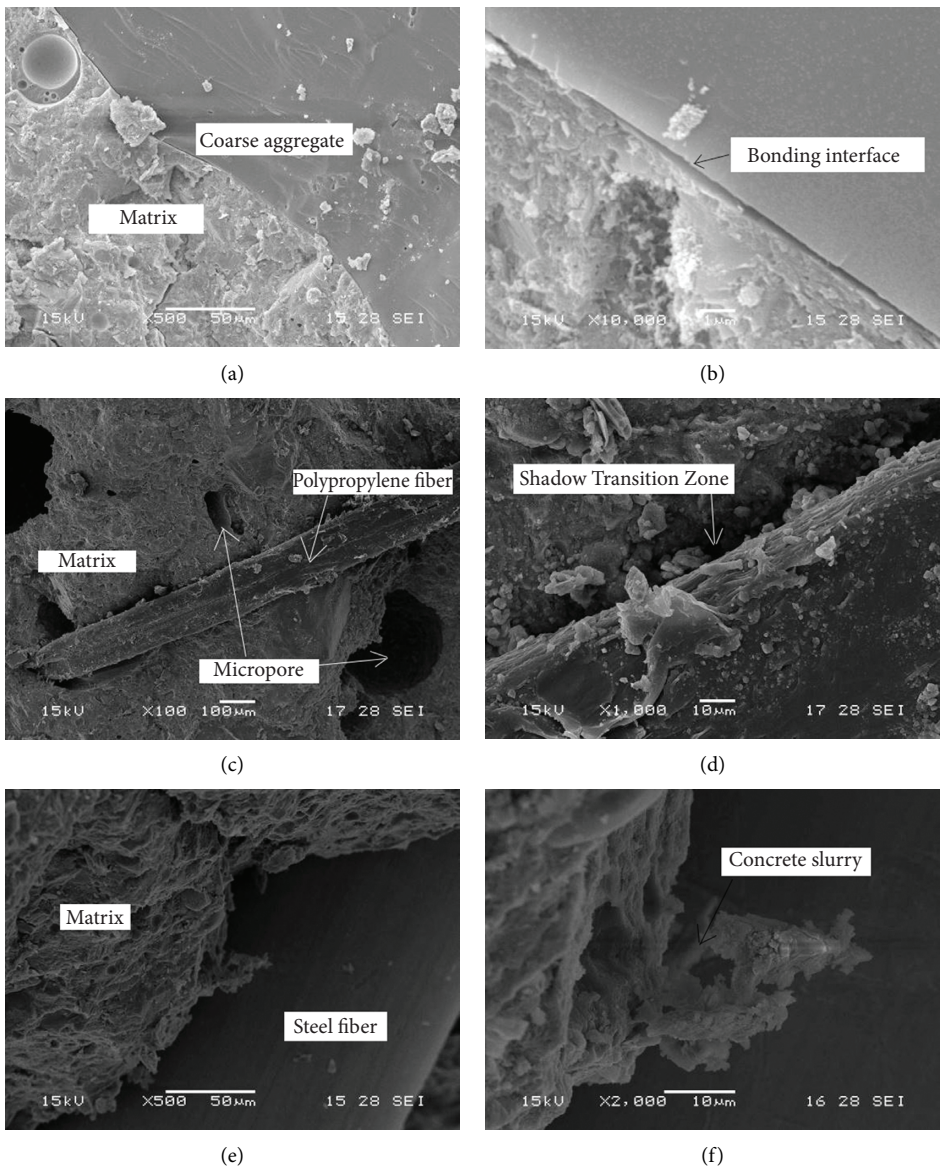

Figure 4: Scanning chart of three different factors and the transition zone of the UHPC matrix; (a) (b) coarse aggregate-UHPC; (c) (d) polypropylene fiber-UHPC; and (e) (f) steel Fiber-UHPC.

improve the bonding effect between the UHPC matrix and the aggregate transition zone. Second, coarse aggregate can form support in UHPC to improve the compressive strength and elastic modulus of UHPC. Richard [21] found that the elastic modulus of UHPC mixed with 630 kg/m3 basalt gravel reached 57 GPa, which was significantly higher than that of ordinary UHPC. The results of this study were consistent with this conclusion.

Figures 4(c) and 4(d) show one polypropylene fiber located in the UHPC matrix and the other exposed outside. It is obvious that the holes near the polypropylene fiber have a large shadow area at the junction of the concrete matrix, which is not as close as that of the coarse aggregate. This is because the air-entraining property of the polypropylene fiber itself leads to an increase in the porosity of the UHPC matrix [22–24]. Polypropylene fiber has a certain interfacial effect due to its soft material, poor tensile performance, and low elastic modulus [25]. When the content is too much, it will play the role of air entraining, thus destroying the compactness of the ultra-high performance concrete matrix and reducing the strength of the ultra-high performance concrete. Only in the case of less content has a small positive effect on compressive and flexural strength.

Figures 4(e) and 4(f) show the details of the bond between steel fiber and the UHPC matrix. Compared with Figures 4(c) and 4(d), the bond between steel fiber and the UHPC matrix is closer. It is obvious that there is no hole near the bond, and the bond between concrete slurry and steel fiber is very tight at the junction. It can be seen that the cement slurry is very strictly attached to the surface of the steel fiber. The strengthening mechanism of steel fiber on the concrete matrix is mainly reflected in the high tensile

strength and elastic modulus of steel fiber, so that steel fiber can play an anchoring role in the concrete matrix and block the development of cracks, reducing the damage to the matrix caused by the rapid cracking of local microcracks, thereby effectively improving the compressive strength of the UHPC matrix.

The results of the scanning electron microscopy test well explain why the incorporation of steel fiber has a high improvement in compressive strength and flexural strength. Kumar Mehta et al. found that the elastic modulus of concrete was mainly related to the elastic materials and the proportion of each component of concrete [26]. The influence of steel fiber on the elastic modulus is mainly the dosage. Some scholars have shown that when the steel fiber content increases from 0% to 3%, the elastic modulus of UHPC increases. However, when the steel fiber content is greater than 4%, the working performance of UHPC decreases sharply due to excessive fiber content, which leads to an increase in internal porosity and a decrease in elastic modulus. Therefore, the content of steel fiber has a certain influence on the elastic modulus of UHPC.

4. Strength Prediction Based on BP Neural Network

4.1. Working Principle of BP Neural Network. The back propagation (BP) neural network is a multilayer feedforward network, which is the most commonly used artificial neural network learning algorithm [27]. According to statistics, nearly 90% of the artificial neural network applications are based on the BP algorithm [28]. The BP neural network is based on its own multilayer perceptron, imitating the reaction process of human brain neurons to external stimuli and using the forward propagation of signals and the reverse adjustment of errors to establish an intelligent network prediction that can effectively deal with nonlinear information. Because of its strong ability to learn and process data, it is widely used in engineering. the BP neural network is generally composed of an input layer, one or more hidden layers, and an output layer. The neural network structure used in this experiment is shown in Figure 5. Each structure layer contains one or more neurons. The adjacent layer neurons are fully connected by adjustable weights. By changing the connection weights or thresholds of the network to adapt to the requirements of the outside world in order to achieve the required error requirements, so as to obtain the most real prediction value. Therefore, the BP neural network has fault tolerance, self-learning ability, and adaptive ability.

4.2. Establishment and Data Processing of Neural Networks. In this paper, the experimental data are randomly divided into a training set, a verification set, and a test set according to 70%, 15%, and 15%. In order to construct the strength prediction model of hybrid fiber UHPC, a three-layer structure neural network system was used. The number of neurons in the input layer was 3. After an empirical formula and multiple experiments, the number of neurons in the hidden layer was 7 and the number of neurons in the output layer was 3. Combined with the MATLAB language program, the neural network toolbox was called, and the new function was used to establish the BP neural network. The pure linear transfer function was used in the input and output layers, and the S-type transfer function was used in the hidden layer. The training number was 3000, the learning rate was 0.01, and the training error target value was 0.00001. Since many measured data are not in the same order of magnitude, in order to avoid the large numerical difference and affect the training accuracy, the training data are normalized to make it between 0 and 1. The normalization formula used in this paper is shown in formula (3).

$$Y = \frac{X - X_{\min}}{X_{\max} - X_{\min}}. \tag{3}$$

In the formula, Y represents the normalized result; $X_{\max}$ is the maximum value in the sample; $X_{\min}$ is the minimum value in the sample; and X is the sample value before normalization. Figure 6 is the fitting of the training set, validation set, test set, and total set after training when the hidden layer is 7 neurons. The correlation between the predicted results and the experimental results is close to 1.

4.3. Verification of Neural Network Model. All the experimental data are imported into the BP neural network model for prediction, and the strength fitting curve is obtained as shown in Figure 7. In this paper, the errors of the BP neural network model in training and testing are comprehensively evaluated by the root mean square error (RMSE), the mean absolute error (MAE), the mean relative error (MAPE), the maximum relative error (MAX-RE), and the goodness of fit coefficient R^2(see Table 9). The calculation formula is as follow:

$$\begin{aligned}
RMSE &= \sqrt{\frac{1}{n}\sum_{i=1}^{n}\left(y_i - \widehat{y}_i\right)^2},\\
MAE &= \frac{1}{n}\sum_{i=1}^{n}\left|y_i - \widehat{y}_i\right|,\\
MAPE &= \frac{1}{n}\sum_{i=1}^{n}\frac{\left|y_i - \widehat{y_i}\right|}{y_i}\times 100\%,\\
\mathrm{MAX}-RE &= \max\left(\frac{\left|y_i - \widehat{y}_i\right|}{y_i}\times 100\%\right),\\
R^2 &= 1 - \frac{\sum_{i=1}^{n}\left(y_i - \widehat{y}_i\right)^2}{\sum_{i=1}^{n}\left(y_i - \bar{y}_i\right)^2}.
\end{aligned} \tag{4}$$

Through the above analysis, it can be found that the BP neural network is used to predict the three strength parameters, and the error analysis of the test data is carried out from different angles. The results show that for the root mean square error and the average absolute error, the

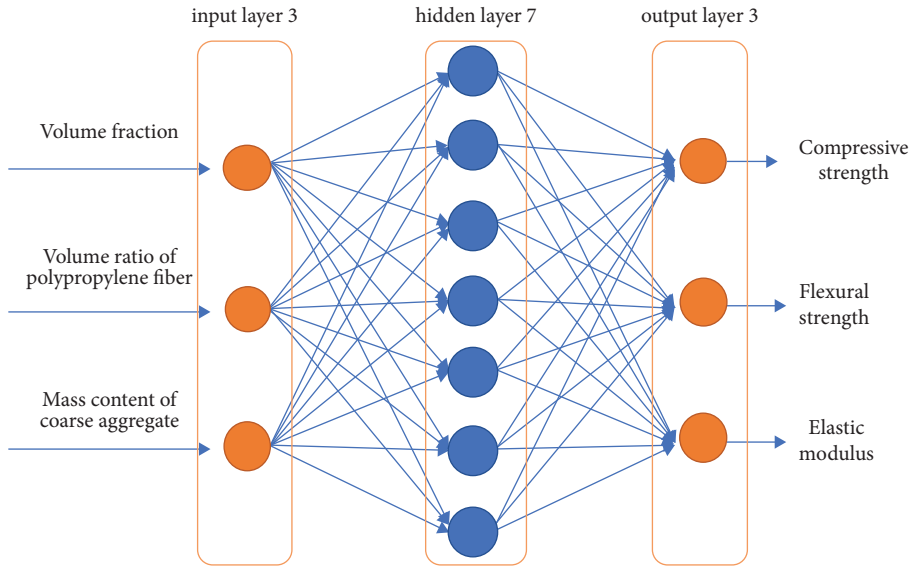

Figure 5: Neural network structure diagram.

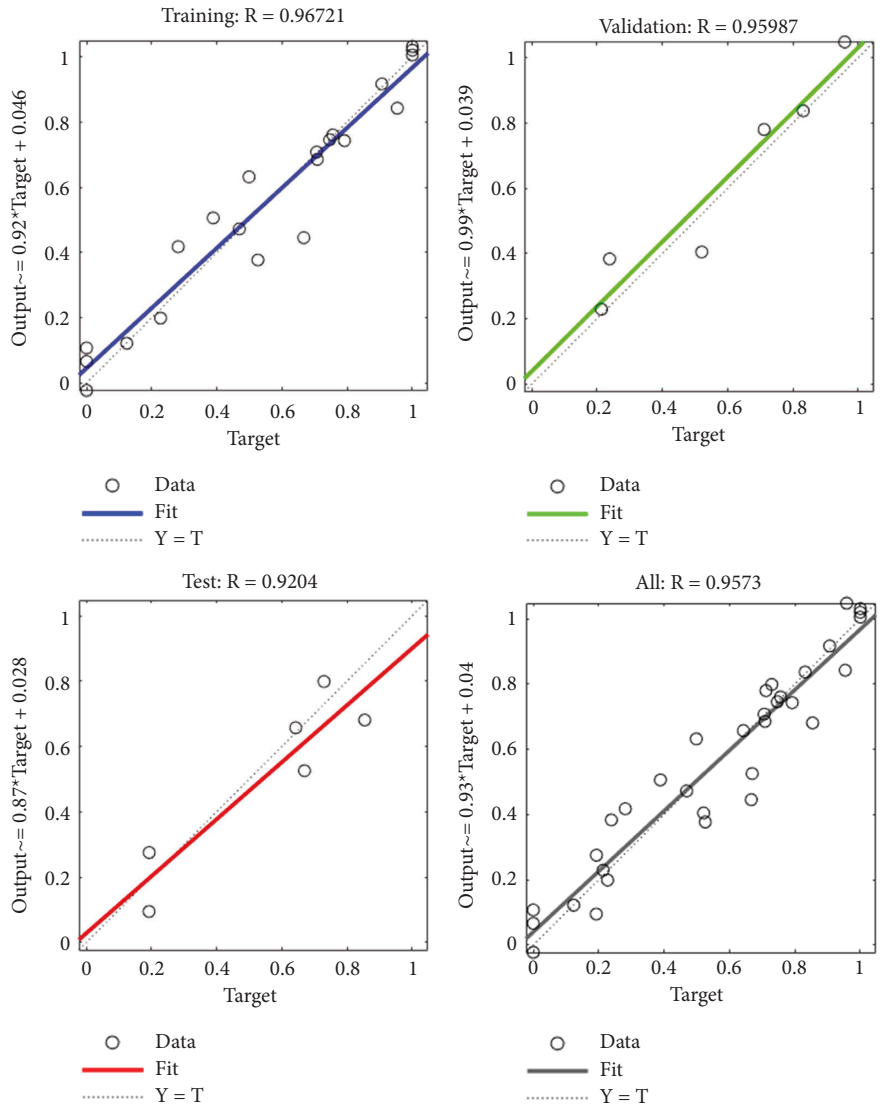

Figure 6: Model 3-7-3 network structure R^2 value.

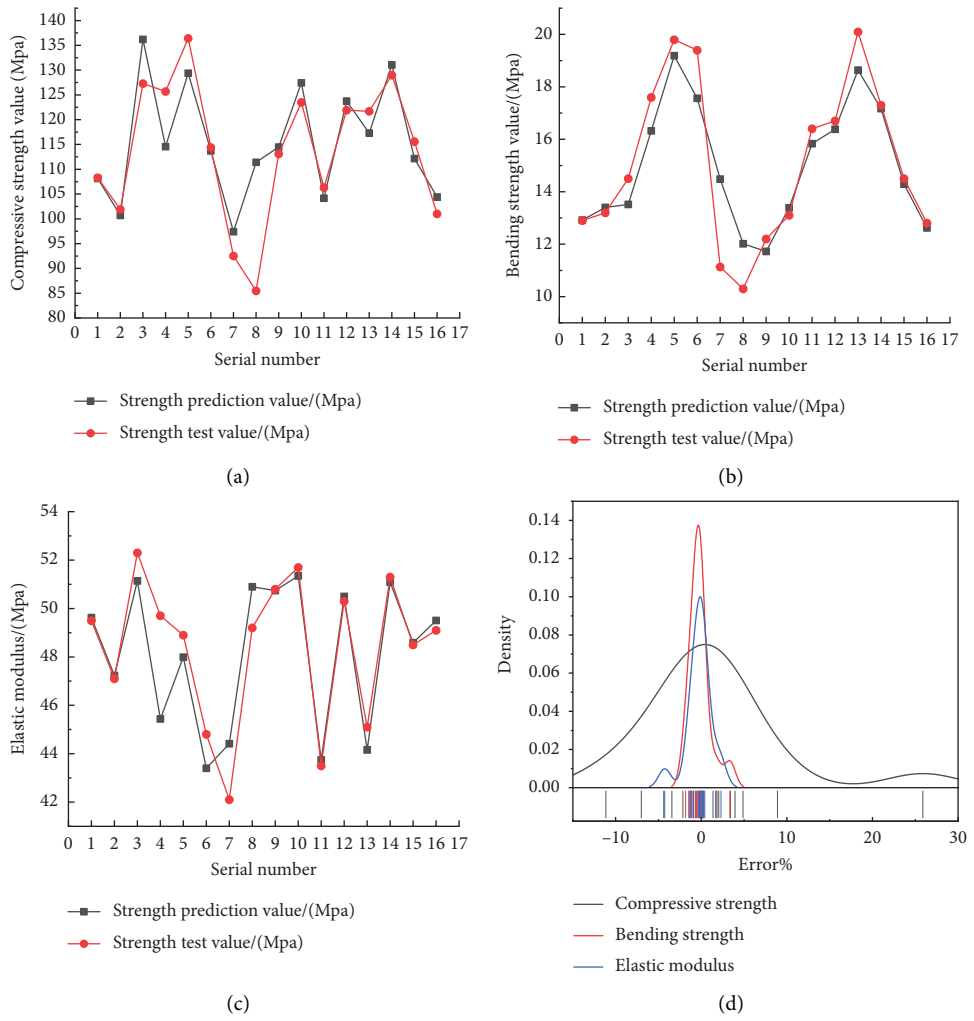

Figure 7: Fitting curve and error distribution of measured and predicted values; (a) prediction curve of compressive strength; (b) prediction curve of bending strength; (c) elastic modulus prediction curve; and (d) distribution of the difference between the predicted value and real value.

Table 9: Error values corresponding to different evaluation methods.

Forecasting model	RMSE	MAE	MAPE (%)	MAX-RE (%)	R^2
Compressive strength	7.99	5.15	5.0	30.0	0.65
Bending strength	1.21	0.85	6.0	30.0	0.84
Elastic modulus	1.41	0.91	2.0	9.0	0.77

prediction error of compressive strength is significantly greater than the prediction errors of bending strength and elastic modulus, and the average relative error is small, and the maximum goodness of fit is 0.84. It can be clearly seen that the difference distribution between the predicted value and the real value approximately obeys the normal distribution, and the error percentage distribution is concentrated in (−5%, 5%), indicating that the BP neural network prediction results selected in this paper are feasible in a certain error allowable range and a have certain prediction value, which has certain reference significance for engineering practice.

5. Conclusions

In this paper, the basic mechanical properties of UHPC-CA were studied by designing three factors and four levels of orthogonal tests. The main conclusions are as follows:

(1) Steel fiber can improve the compressive performance, bending performance, and elastic modulus of the cube. When the volume ratio of steel fiber was 1.5%, the three indexes reached their maximum value. When the mass replacement rate of the coarse aggregate is not more than 15%, the compressive

strength of UHPC-CA increases with the increase of the coarse aggregate replacement rate, and the elastic modulus also increases greatly. However, when the value is greater than 15%, the compressive strength of UHPC-CA is reduced to a certain extent, and the bending strength is also negatively affected. When the volume fraction of polypropylene fiber is not greater than 0.10%, the compressive strength and flexural strength increase slightly, and the influence on the elastic modulus can be ignored. When the polypropylene fiber content is greater than 0.10%, the strength of UHPC-CA decreases because of its own air-entraining property.

(2) Through range analysis, variance analysis, factor intuitive analysis, and factor weight analysis based on AHP and entropy weight method, the influence ranking of each factor level on the experimental results is obtained. Through the study of the fiber mixing effect, the optimal mix ratio for the experiment is determined as A2B3C4, namely, the mass content of coarse aggregate is 15%, the volume content of polypropylene is 0.1%, and the volume content of steel fiber is 1.5%.

(3) Through the SEM scanning of UHPC, the influence of various factors on the experiment was reasonably explained from the microscopic point of view, and the authority of the optimal mix ratio was further verified.

(4) Based on the BP neural network, the strength parameters of UHPC can be well predicted. The relative error percentage between the predicted value and the true value is between (−5%, 5%), and the goodness of fit is close to 1. The prediction effect is relatively good, which can provide some reference for the mix design of ultra-high performance concrete with coarse aggregate.

Data Availability

All data included in this study are available from the corresponding author upon rerequest.

Conflicts of Interest

The authors declare that they have no conflicts of interest.

Acknowledgments

The funding for this investigation was provided by the National Natural Science Foundation of China (Grant no. 51878518). The authors greatly appreciate their financial support.

References

[1] K. Wille and A. E. Naaman, "Ultra-high performance concrete with compressive strength exceeding 150 MPa (22 ksi): a simpler way," *ACI Materials Journal*, vol. 108, no. 1, pp. 46–54, 2011.

[2] H. Hong, "Application and economic analysis of ultra-high performance concrete," *Building Science and Technology*, vol. 5, no. 3, pp. 32–35, 2021.

[3] B. X. Li, *Study on Preparation of Low-Cost Environment-Friendly Ultra-high Performance concrete*, School of Civil Engineering, Changsha, China, 2009.

[4] W. R. Huang, Y. Z. Yang, and T. Cui, "Study on shrinkage and deformation properties of ultra-high performance concrete containing coarse aggregate," *Concrete*, vol. 43, no. 8, pp. 99–103, 2021.

[5] B. Xu and H. C. Song, "Hybrid effect of hybrid fiber composites," *Acta Compositae Sinica*, vol. 1, pp. 67–95, 1988.

[6] L. H. Xu, B. Li, and Y. Chi, "Study on stress-strain relationship of steel-polypropylene hybrid fiber concrete under uniaxial cyclic compression," *Journal of Architectural Structure*, vol. 39, no. 4, pp. 140–152, 2018.

[7] X. Q. Kong, H. D. Gao, and J. M. Gang, "Study on flexural toughness of steel-polypropylene hybrid fiber recycled concrete," *Silicate Bulletin*, vol. 37, no. 9, pp. 2729–2736, 2018.

[8] N. A. Libre, M. Shekarchi, M. Mahoutian, and P. Soroushian, "Mechanical properties of hybrid fiber reinforced lightweight aggregate concrete made with natural pumice," *Construction and Building Materials*, vol. 25, no. 5, pp. 2458–2464, 2011.

[9] J. J. Yu, B. S. Zhang, W. Z. Chen, and H. Liu, "Multi-scale analysis on the tensile properties of UHPC considering fiber orientation," *Composite Structures*, vol. 280, Article ID 114835, 2022.

[10] H. Huang, X. Gao, L. Li, and H. Wang, "Improvement effect of steel fiber orientation control on mechanical performance of UHPC," *Construction and Building Materials*, vol. 188, no. 188, pp. 709–721, 2018.

[11] H. Huang, X. Gao, and K. H. Khayat, "Contribution of fiber orientation to enhancing dynamic properties of UHPC under impact loading," *Cement and Concrete Composites*, vol. 121, Article ID 104108, 2021.

[12] Z. C. Deng and Q. Feng, "Fracture properties of hybrid fiber reactive powder concrete," *Journal of Building Materials*, vol. 19, no. 1, pp. 14–21, 2016.

[13] Z. C. Deng and R. D. Jumbe, "Experimental study on toughening characteristics of mixed fiber RPC," *Journal of Building Materials*, vol. 18, no. 2, pp. 202–207, 2015.

[14] Z. C. Deng, "Flexural toughness and evaluation method of hybrid fiber reinforced ultra-high performance concrete," *Journal of Composite Materials*, vol. 33, no. 6, pp. 1274–1280, 2016.

[15] *Standard for Test Methods of Mechanical Properties of Ordinary Concrete GB/T50081-2002*, China Academy of Building Research, Beijing, 2007.

[16] J. Cheng, J. P. Liu, and J. Z. Liu, "Study on mechanical properties and mechanism analysis of ultra-high performance concrete containing coarse aggregate," *Material Guide*, vol. 31, no. 23, pp. 115–131, 2017.

[17] J. W. Guo, X. Q. Pu, and X. Gao, "An improved method for calculating index weight of multi-objective decision-making," *Journal of Xidian University*, vol. 41, no. 6, pp. 118–125, 2014.

[18] Q. Y. Cheng, "Structural entropy weight method for determining the weight of evaluation index," *Theory and Practice of System Engineering*, vol. 30, no. 7, pp. 1225–1228, 2010.

[19] C. Xu, "Influence of fiber hybrid effect on mechanics and durability of concrete composites," *Functional Materials*, vol. 52, no. 1, pp. 1202–1207, 2021.

[20] Z. J. Wang, Z. Q. Wei, and G. P. Zhu, "Early cracking resistance of composite fiber reinforced concrete," *Railway Construction*, vol. 60, no. 5, pp. 145–149, 2020.

[21] P. Richard, "Reactive power concrete: a new ultra-high strength cemented material," in *The 4th International Symposium on Utilization or High Strength/High Performance Concrete*Spriger, Paris, 1996.
[22] J. J. Zhang, G. Z. Zhao, and Y. Y. Zhao, "Study on tensile strength of reactive powder concrete with different fibers," *Journal of North University of China (Natural Science Edition)*, vol. 37, no. 3, pp. 318–322, 2016.
[23] Q. Chen, "Effect of polypropylene fiber and coarse aggregate on tensile strength of ultra-high performance concrete," *Journal of Hydraulic and Building Engineering*, vol. 17, no. 6, pp. 113–116, 2019.
[24] Q. Chen, L. H. Xu, F. H. Wu, Y. Q. Zeng, and X. Y. Liang, "Experimental study on strength of steel-polypropylene hybrid fiber reinforced ultra-high performance concrete," *Silicate Bulletin*, vol. 39, no. 3, pp. 740–748, 2020.
[25] L. H. Xu, D. T. Xia, G. Z. Xia, and Y. Chi, "Effects of steel fiber and polypropylene fiber on strength of high strength concrete," *Journal of Wuhan University of Technology*, vol. 4, pp. 58–60, 2007.
[26] K. Mehta and P. J. M. Montero, *Microstructure, properties and materials of concrete*, China Electric Power Press, China, 2008.
[27] H. Erdal, M. Erdal, O. Simsek, and H. I. Erdal, "Prediction of concrete compressive strength using non-destructive test results," *Computers and Concrete*, vol. 21, no. 4, pp. 407–417, 2018.
[28] Y. Shi and K. H. Fang, "Neural network prediction method for RCC durability," *Papers of the Fifth International Symposium on RCC Dams*, vol. 1, Guizhou, China, 2007.